Gd3+ Complexes Conjugated to Cyclodextrins: Hydroxyl Functions Influence the Relaxation Properties

Anais Biscotti, François Estour, Berthe-Sandra Sembo-Backonly, Sebastien Balieu, Michaël Bosco, Cécile Barbot, Agnes A. Pallier, Éva Tóth, Celia Bonnet, Géraldine Gouhier

processes

MDPI

Article

Gd^{3+} Complexes Conjugated to Cyclodextrins: Hydroxyl Functions Influence the Relaxation Properties

Anais Biscotti [1], François Estour [1], Berthe-Sandra Sembo-Backonly [1], Sébastien Balieu [1], Michaël Bosco [1], Cécile Barbot [1], Agnès Pallier [2], Éva Tóth [2], Célia S. Bonnet [2,*] and Géraldine Gouhier [1,*]

[1] Normandie Université, COBRA, UMR 6014, FR 3038, INSA Rouen, CNRS, IRIB, IRCOF, 1 rue Tesnière, 76821 Mont Saint Aignan, France; anais.biscotti@gmail.com (A.B.); Francois.estour@univ-rouen.fr (F.E.); sandra.sembo-backonly@etu.univ-rouen.fr (B.-S.S.-B.); sebastien.balieu@univ-rouen.fr (S.B.); mik_bosco@yahoo.fr (M.B.); cecile.barbot@univ-rouen.fr (C.B.)

[2] Centre de Biophysique Moléculaire, CNRS UPR 4301, Université d'Orléans, Rue Charles Sadron, CEDEX 2, 45071 Orléans, France; agnes.pallier@cnrs-orleans.fr (A.P.); eva.jakabtoth@cnrs-orleans.fr (É.T.)

* Correspondence: celia.bonnet@cnrs-orleans.fr (C.S.B.); geraldine.gouhier@univ-rouen.fr (G.G.); Tel.: +33-238-255-593 (C.S.B.); +33-235-522-909 (G.G.)

Abstract: In the search for improvement in the properties of gadolinium-based contrast agents, cyclodextrins (CDs) are interesting hydrophilic scaffolds with high molecular weight. The impact of the hydrophilicity of these systems on the MRI efficacy has been studied using five β-CDs substituted with DOTA or TTHA ligands which, respectively, allow for one (q = 1) or no water molecule (q = 0) in the inner coordination sphere of the Gd^{3+} ion. Original synthetic pathways were developed to immobilize the ligands at C-6 position of various hydroxylated and permethylated β-CDs via an amide bond. To describe the influence of alcohol and ether oxide functions of the CD macrocycle on the relaxation properties of the Gd^{3+} complexes, ^{1}H Nuclear Magnetic Relaxation Dispersion (NMRD) profiles, and ^{17}O transverse relaxation rates have been measured at various temperatures. The differences observed between the hydroxylated and permethylated β-CDs bearing non-hydrated GdTTHA complexes can be rationalized by a second sphere contribution to the relaxivity in the case of the hydroxylated derivatives, induced by hydrogen-bound water molecules around the hydroxyl groups. In contrast, for the DOTA analogs the exchange rate of the water molecule directly coordinated to the Gd^{3+} is clearly influenced by the number of hydroxyl groups present on the CD, which in turn influences the relaxivity and gives rise to a very complex behavior of these hydrophilic systems.

Keywords: cyclodextrin; gadolinium; contrast agent; magnetic resonance imaging; second hydration sphere

Citation: Biscotti, A.; Estour, F.; Sembo-Backonly, B.-S.; Balieu, S.; Bosco, M.; Barbot, C.; Pallier, A.; Tóth, É.; Bonnet, C.S.; Gouhier, G. Gd^{3+} Complexes Conjugated to Cyclodextrins: Hydroxyl Functions Influence the Relaxation Properties. *Processes* **2021**, *9*, 269. https://doi.org/10.3390/pr9020269

Academic Editor: Francesco Parrino
Received: 18 December 2020
Accepted: 26 January 2021
Published: 30 January 2021

1. Introduction

Magnetic resonance imaging (MRI) is currently used to diagnose diseases and to monitor treatment progress in deep tissues. This noninvasive technique is based on the measurement of nuclear spin relaxation times of water protons of the organism. MR images are obtained thanks to the variation of the longitudinal or the transverse relaxation times (T_1- or T_2-weighted images, respectively) between different tissues [1–3]. In order to improve the image contrast and reduce the examination time, contrast agents are commonly injected to patients. These compounds are stable gadolinium chelates formed with polyamino-polycarboxylate ligands, such as the macrocyclic GdDOTA (H_4DOTA = 1,4,7,10-tetraazacyclododecane-1,4,7,10-tetraacetic acid). Via dipole–dipole interactions between the water proton spins and the electron spin of Gd^{3+}, such paramagnetic complexes induce an acceleration of the proton spin relaxation. In the GdDOTA chelate, the metal ion is nine-coordinated with one water molecule in the inner coordination sphere (IS), q = 1. The presence of this water molecule, directly coordinated to Gd^{3+}, is important for an efficient

relaxation effect [4–6]. Indeed, its exchange with surrounding water molecules transmits the paramagnetic effect of the Gd^{3+} to bulk water, which is then detectable on the MR images. In the absence of inner sphere coordination water, a Gd^{3+} complex has a more limited effect on the water proton relaxation times.

The efficiency of a T_1 contrast agent is assessed by its longitudinal relaxivity, r_1, defined as the paramagnetic relaxation rate enhancement referred to 1 mM concentration of the metal ion. A high r_1 value translates to good contrast enhancing capability in MR imaging. Relaxivity is influenced by different relaxation mechanisms [7]. Inner sphere relaxivity arises from the interaction of the Gd^{3+} electron spin with the inner sphere water protons and their exchange with bulk water. This mechanism is described by the theory of Solomon, Bloembergen, and Morgan for paramagnetic nuclear relaxation, which relates the relaxivity to microscopic parameters of the Gd^{3+} complex, such as the hydration number q, the water exchange rate k_{ex}, and the rotational correlation time τ_r [8,9]. The outer sphere (OS) relaxation mechanism originates from interactions of the Gd^{3+} electron spin with water molecules randomly diffusing around the complex. Finally, a second sphere (2S) mechanism might be also operating for systems containing water molecules strongly hydrogen-bonded to the functional groups of the complex. This second sphere effect is usually negligible, and it is difficult to describe when it exists. The contribution of each mechanism to the relaxivity depends on the structure of the complex, especially the size, the presence of hydrogen bonding acceptors, the charge, and the hydrophilicity. Commercial contrast agents are small, monohydrated Gd^{3+} complexes of polyamino-polycarboxylate ligands for which the IS and OS relaxivity contributions are similar. With an appropriate chemical design, the inner and second sphere contributions can be substantially increased, while the outer sphere relaxivity can practically not be modified.

The inner sphere relaxivity term is linearly proportional to the hydration number. Therefore, increasing q is a straightforward way to improve relaxivity. However, the presence of two or more inner sphere water molecules in the complex can seriously compromise its stability, thereby increasing the potential risk of releasing free and toxic Gd^{3+} [10–12]. Relaxivity can be also increased by optimizing the water exchange rate and the rotational motion time of the complex. The rate of water exchange is correlated with the exchange mechanism. The majority of the polyamino-polycarboxylate complexes of Gd^{3+} undergo a dissociative exchange, i.e., the leaving of the bound water molecule precedes the entering of the incoming water molecule. In this case, the steric hindrance around the water binding site and the global charge of the complex are important parameters to determine the exchange rate, and water exchange can be accelerated by increasing the steric hindrance around the water binding site. The most common way to reach higher relaxivity, with major improvements at medium frequencies (20–60 MHz), has been to increase the rotational correlation time, τ_r, by increasing the molecular weight of the complex. Indeed, for low molecular weight complexes, fast rotation limits the relaxation efficiency. Thus, a large number of bulkier ligands coordinating the Gd^{3+} ion was developed to create more efficient MRI contrast agents. Gd^{3+} complexes were therefore incorporated into macromolecular systems such as proteins [12–15], dendrimers [16], cyclodextrins [17], polyrotaxanes [18–20], etc. However, the relaxivity enhancements has been often less than those expected, due to the flexibility of the macromolecule which implies faster local motion for Gd^{3+} than the overall slow motion of the entire macromolecule.

We have focused our study on cyclodextrins (CDs) as interesting and versatile scaffolds to design potential MRI contrast agents. CDs are natural cyclic oligosaccharides with 6, 7, or 8 glucose units, issued from starch degradation by glucosyltransferase (CGTase) and so-called α-, β-, and γ-CD, respectively [21]. Cyclodextrins have primary (C-6) and secondary hydroxyl groups (C-2, C-3) forming the smaller and larger crowns of the cone, respectively. For β-CD, this cone shape is especially reinforced by hydrogen bonding between two adjacent units (C-2-OH and C-3-OH). The 21 alcohol functions also favor interactions with water molecules and improve the solubility in aqueous medium. The internal cavity (host), composed of glycosidic oxygen and C-H groups, is less hydrophilic

and makes possible intermolecular interactions with organic molecules (guests). Host–guest inclusion complexes improve the water solubility and the stability of the guests, such as small bioactive molecules. In the context of MRI contrast agents, cyclodextrins have been mainly explored in three distinct approaches in the objective of modulating the rotational motion, thus improving relaxivity: (i) as host to form inclusion complexes with contrast agents functionalized by lipophilic groups [22–24], (ii) as high molecular weight scaffolds by covalently immobilizing one or more Gd^{3+} complexes [25,26], and (iii) as a platform for Ln^{3+} complexation [27,28].

In the first two approaches, dimers, trimers [23], polymers [29], and polyrotaxanes [18–20] of CDs were developed in order to maximize the number of Gd^{3+} complexes per molecule. For the development of platform for Ln^{3+} complexation, CDs were modified, for instance, into per-3,6-anhydro derivatives, which affected their structure leading to a hydrophilic cavity capable of metal binding. The replacement of the hydroxyl groups by carboxylate functions gives a ligand, which can complex hard Ln^{3+} ions to form mono- and bimetallic species [27]. The relaxivity of the monometallic Gd^{3+} has been investigated in details using a rigorous approach, where a maximum of the microscopic parameters was determined independently. It has been demonstrated that the high relaxivity obtained was due to the high hydration number of the complex and a relatively long rotational correlation time explained by the hydrophilic character of the complex [28].

6-*O*-Peracetylated-β-CDs were also synthesized to coordinate Gd^{3+} in the axis of the macrocycle [30–32]. In particular, the effect of the second hydration sphere has been studied using the native and permethylated CDs. It has been proved that this functionalization had an impact on the relaxivity. Indeed, a 40% relaxivity enhancement was observed with perhydroxylated β-CDs (4.6 mM^{-1} s^{-1} and 6.5 mM^{-1} s^{-1}, respectively). As these complexes had similar structure and identical hydration number (q = 2), the relaxivity difference was attributed to the presence of hydrogen-bound water molecules around the hydroxyl groups inducing an important second-sphere (2S) contribution to relaxivity.

In order to improve the thermodynamic stability of the Gd^{3+} chelate and further study the influence of the hydrogen-bonding network provided by the hydrophilic cyclodextrins on the relaxivity, several functionalized cyclodextrins were synthesized and studied. Modified DOTA and TTHA (3,6,9,12-tetrakis(carboxymethyl)-3,6,9,12-tetraazatetradecane-1,14-dioic acid) ligands were conjugated at one of the C-6 position of various β-CDs by replacing a carboxylate function by an amide (**1**–**5**, Figure 1).

The DOTA monoamide (DOTAMA) ligand is known to form thermodynamically stable and kinetically inert complexes with Ln^{3+}. The GdDOTAMA complex was introduced at one of the *O*-6-position on the small rim of the native (hydroxylated) β-CD (**1**), of the 6-*O*-permethylated β-CD (**2**), and of the 2,3,6-*O*-permethylated β-CD (**3**). With contrast agent **2**, the hydroxyl groups are in the vicinity of the GdDOTAMA complex, while the methoxy groups are located on the opposite side on the larger rim of the CD. In order to better decipher the relaxation behavior of those compounds, TTHA monoamide (TTHAMA) was also introduced on the native (**5**) and 2,3,6-*O*-permethylated β-CD (**4**) (Figure 1). TTHA is a commercially available linear ligand with six carboxylic acid and four amine functions which can chelate the Gd^{3+} ion. This full coordination by the ligand prevents inner sphere (IS) binding of any water molecule. Indeed, the Gd^{3+} complex of TTHAMA has no inner sphere hydration water molecule (q = 0), which means that the relaxivity will be governed by outer sphere, and possibly second sphere mechanisms [33].

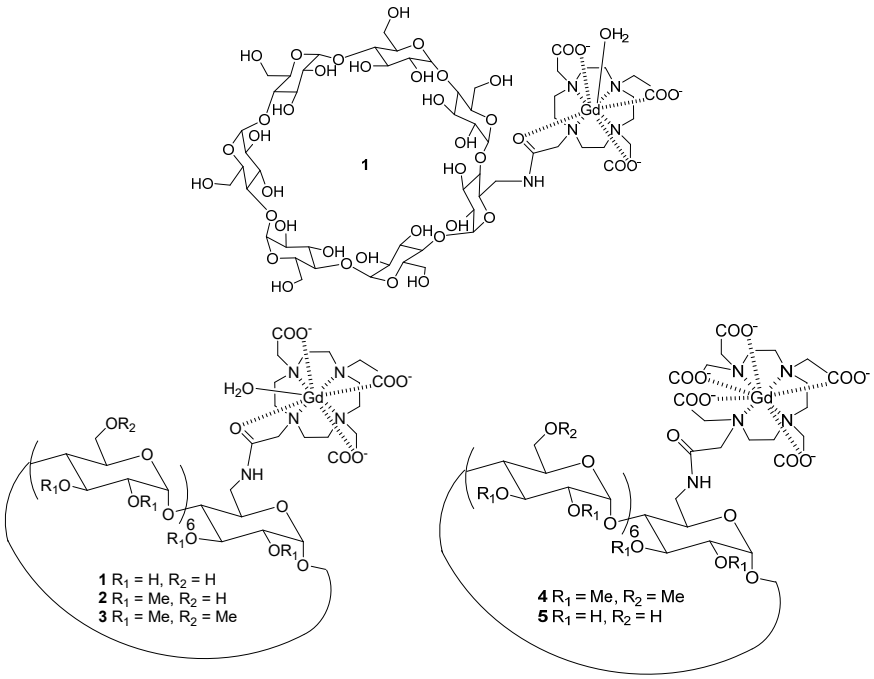

Figure 1. Structure of new contrast agents based on β-CDs-DOTAMA (**1**–**3**) and β-CDs-TTHAMA (**4** and **5**) ligands.

2. Results and Discussion

2.1. Synthesis of CDs Functionalized with DOTA Ligand

The monofunctionalization of native β-CD **6** was based on the difference of reactivity between the hydroxyl groups (Scheme 1). Indeed, the secondary alcohols are more acidic: the position 3 less accessible. We substituted the more nucleophile primary alcohol at 6 position to keep the larger cavity available to form inclusion complex. We reported herein the introduction of DOTA and TTHA ligands on native and methylated-β-CDs.

All synthesis used the same precursor mono(6-amino-6-deoxy)-β-CD **7** obtained after monotosylation of primary face of β-CD **6** and substitution reaction by sodium azide (Scheme 1) [34]. The CD **7** was permethylated after deprotonation and treatment with methyl iodide (Supplementary Materials). The synthesis of the mono(6-azido-6-deoxy)-6-*O*-permethylated-β-CD **9** required two additional steps, the protection of secondary alcohol functions by *tert*-butyldimethylsilyl groups and the deprotection using ammonium fluoride reagent (Supplementary Materials).

The azide reduction using Staudinger reaction led to mono(6-amino-6-deoxy)-β-cyclodextrins precursors **10**–**12** with yields between 40–52%, which was confirmed by the disappearance of the signal in IR spectroscopy of azide function at 2199 cm^{-1} and appearance of amine function at 2920 cm^{-1}. A shift of 10 ppm corresponding to the methylene carbon bearing the amine function was observed by ^{13}C DEPT confirming the reduction step (Supplementary Materials). A peptide coupling was then applied with DOTA structure **13** protected by three *tert*-butyl groups (Scheme 1) [35]. The activation of the free acid function in presence of DCC and HOBt led to the three precursors **14**–**16** in 21%, 12%, and 70% yields, respectively. In order to improve the yields, uronium salt HATU was tested but it did not improve the reactivity [36]. Consequently, another strategy has been developed using the activation of the primary amine function by chloroacetyl chloride reagent (Scheme 2). However, only the permethylated β-CD **12** was substituted in this case in 82% yield. In the case of mono(6-amino-6-deoxy)-perhydroxylated β-CD **10** and mono(6-amino-6-deoxy)-2,3-*O*-permethylated-β-CD **11**, the reactions led to many secondary products due to polysubstitution reactions of the alcohol functions. In order to control the monosubstitution reaction, other precursors **17** and **18** have to be used (Scheme 2).

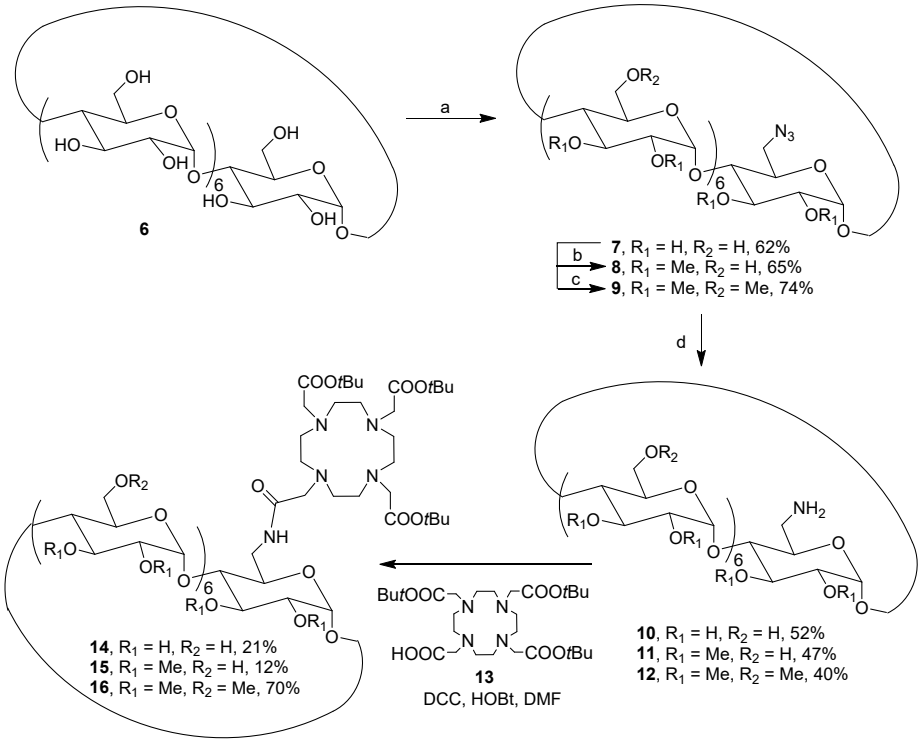

Scheme 1. Synthesis route of 6-*O*-monoamino-β-cyclodextrins precursors **10**–**12** and DOTAMA derivatives **14**–**16**.

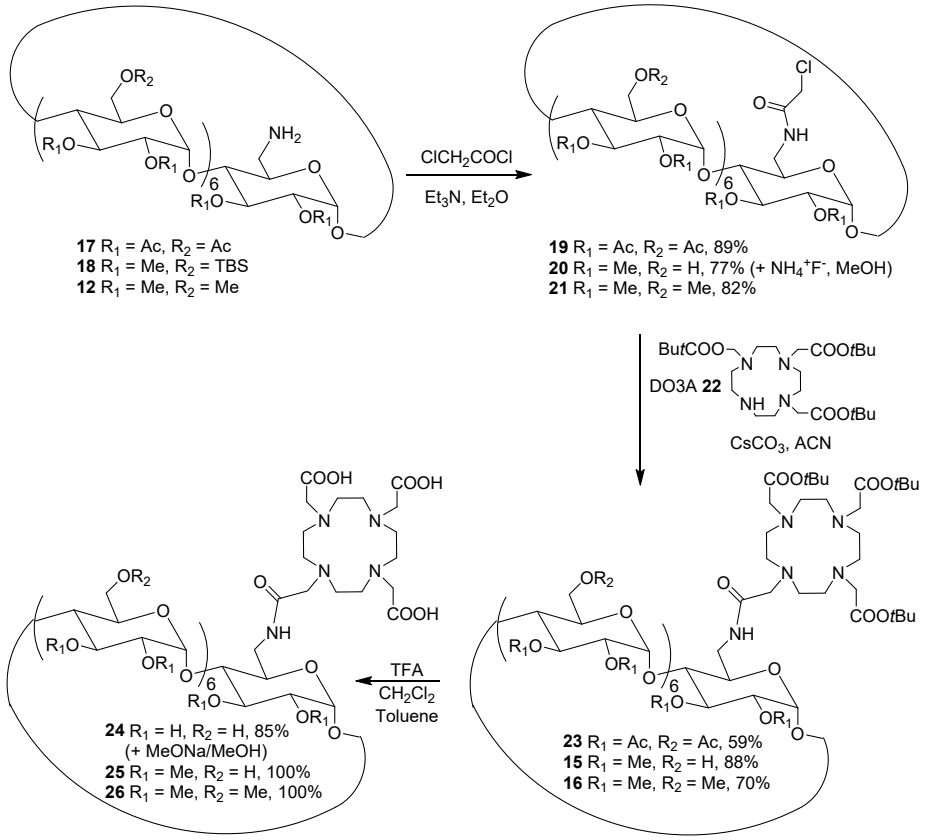

Scheme 2. Second strategy to the synthesis of β-CDs-DOTAMA ligands **24**–**26**.

Thus, the mono(6-amino-6-deoxy)-β-CD **7** was quantitatively peracetylated using anhydride acetic in pyridine and the azido function was then reduced by catalytic hydrogenation in 50% yield (see Scheme 1 in experimental section) (Supplementary Materials). From the same precursor **7**, the mono(6-amino-6-deoxy)-2,3-permethyl-β-CD protected with silyl groups at 6 positions **18** was obtained in three steps by silylation of the residual primary alcohols of the intermediate mono(6-azido-6-deoxy)-β-CD **7** (Scheme 1), followed by a permethylation of the secondary face and after Staudinger reduction of azido group in 51% over yield (see Scheme 2 in experimental section) (Supplementary Materials). The two mono(6-amino-6-deoxy)-CDs **17** and **18** were substituted with chloromethylacetyl group in 89% and 77% yields, respectively (Supplementary Materials). From precursor **18**, an additional deprotection step of the TBS group was required using ammonium fluoride, providing quantitatively compound **20** (see Scheme 3 in experimental section) (Supplementary Materials). The coupling was carried out from the free secondary amine of the commercially available DO3A derivative **22** bearing three *tert*-butylester groups. The DOTAMA ligand was introduced with yields varying between 59% and 88% leading the compounds **23**, **15**, and **16**, thereby improving the initial yields obtained with the direct strategy (21% and 12% yields for **14** and **15**, respectively) (Schemes 1 and 2).

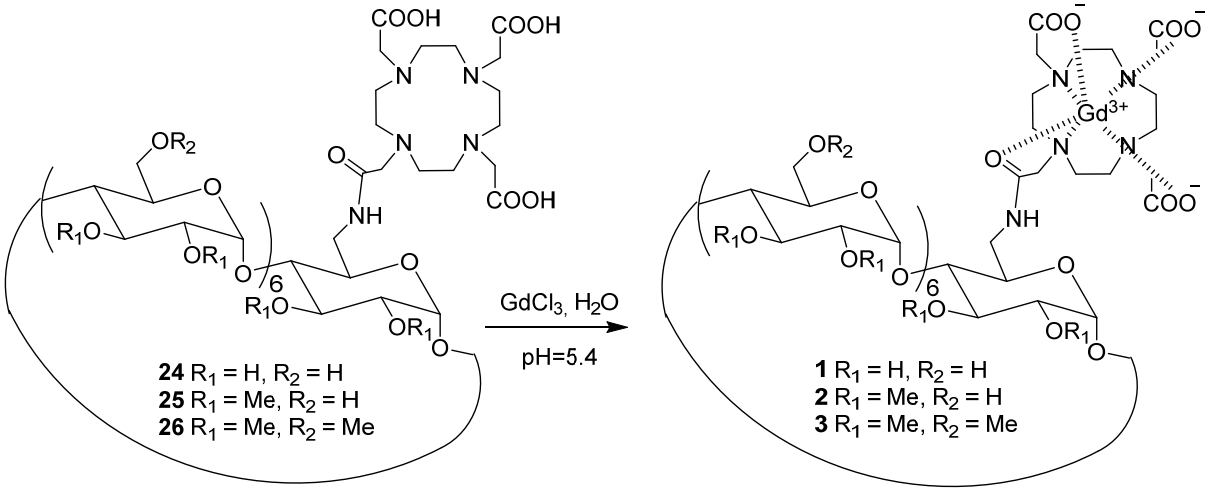

Scheme 3. Formation of β-CD(OH)-GdDOTAMA **1**, β-CD(OH)(OMe)-GdDOTAMA **2**, and β-CD(OMe)-GdDOTAMA **3**.

The ^{1}H NMR spectra confirmed that the substitution of DOTAMA on **15**, **16**, and **23** compounds was effective by the presence of *tert*-butyl groups clearly observed at 1.45 ppm; the other signals being hidden by those of the CD scaffold (Supplementary Materials). For example, the ^{13}C NMR spectrum of precursor **19** revealed a characteristic peak at 42.6 ppm corresponding to the carbon at alpha position of chlorine atom. This signal disappeared in the DOTAMA-substituted **23** and the *tert*-butyl groups signals appeared at 81.8 and 28.0 ppm, respectively. Finally, the methylene groups of the DOTAMA ligand were observed between 55.7 and 62.7 ppm (N-CH_2-CH_2-N and CH_2-COOH) proving the substitution reaction. All the structural analysis was confirmed by mass spectrometry analyses (Supplementary Materials).

The ester functions of compounds **23**, **15**, and **16** were quantitatively deprotected using trifluoroacetic acid in a mixture of dichloromethane/toluene (1/1). In the case of the peracetylated-6-*O*-mono-DOTAMA-β-CD **23**, an additional step using sodium methanoate in methanol was necessary to obtain the hydroxylated CD **24** after a treatment on proton exchange anion resin. The mass spectrometry analyses and the disappearance of *tert*-butyl and acetyl protecting groups on ^{13}C NMR spectrum confirmed the structures **24**–**26** (Supplementary Materials).

Finally, Gd^{3+} complexes of ligands **24**–**26** were prepared in the presence of one equivalent of gadolinium chloride hexahydrate in aqueous medium at pH 5.4 (Scheme 3).

2.2. Synthesis of CDs Functionalized with TTHA Ligand

In order to immobilize TTHA on CD **12**, one carboxylic acid function was activated using one equivalent of HBTU reagent in presence of triethylamine (Scheme 4). The corresponding compound **27** was obtained in 65% yield.

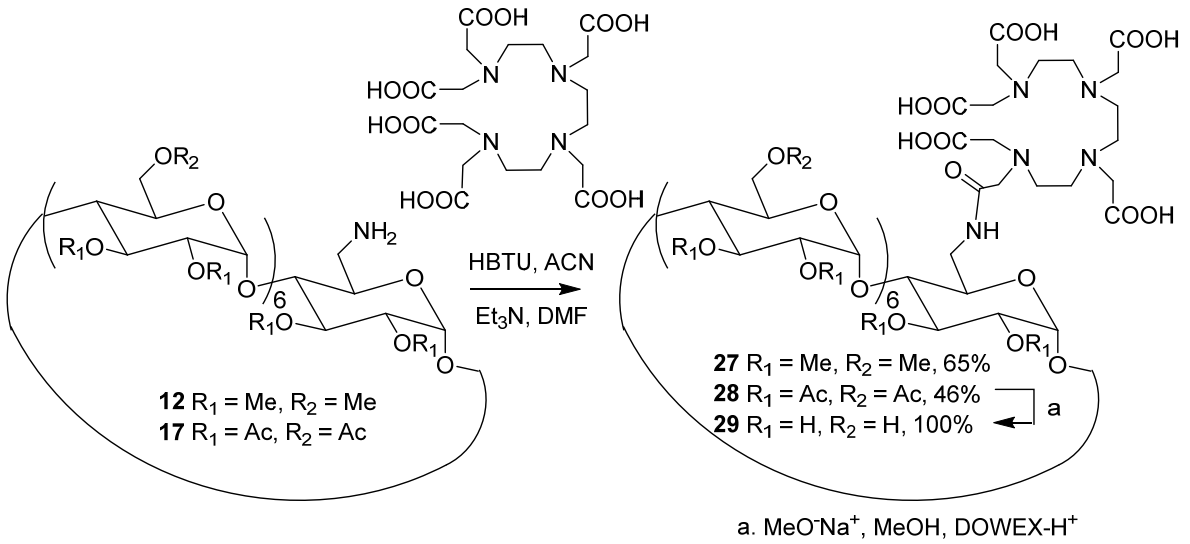

Scheme 4. Formation of β-CDs-TTHAMA **27** and **29**.

As the direct substitution of the perhydroxylated 6-*O*-monoamino-β-CD **10** did not occur (Scheme 1), the peracetylated derivated **17** having a higher solubility in organic solvents was tested. The introduction of the ligand was then possible with 46% yield. This result was confirmed by ^{13}C NMR spectrometry thanks to the characteristic signals of carbonyl function at 171 ppm and the methylene groups of the TTHAMA ligand (57.5–52.5 ppm) (Supplementary Materials). The mass spectrometry analysis was in accordance with the structure **28** (Supplementary Materials). The perhydroxylated compound **29** was obtained quantitatively by basic treatment and purification on Dowex column. The disappearance of the acetyl signals at 21.6 ppm was observed by ^{13}C NMR and the molecular peak at m/z = 1610.6 $[M + H]^+$ confirmed the structure (Supplementary Materials).

Finally, CD-GdTTHAMA **4** and CD(OH)-GdTTHAMA **5** were obtained by addition of gadolinium chloride hexahydrate under controlled pH (Scheme 5).

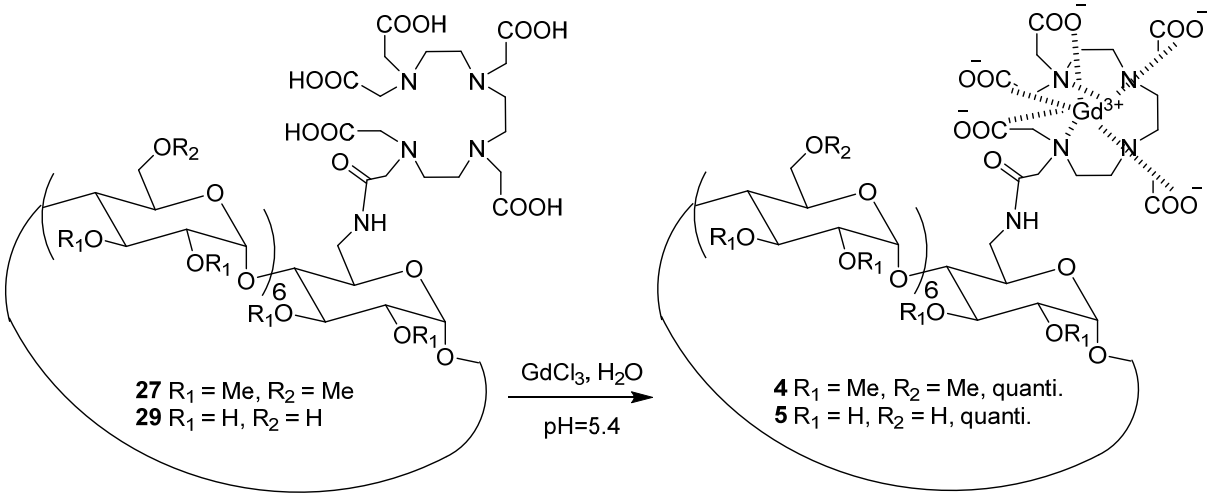

Scheme 5. Formation of β-CD(OMe)-GdTTHAMA **4**, β-CD(OH)-GdDOTAMA **5**.

2.3. Relaxometric Analysis of the TTHA-Derived Complexes **4** *and* **5**

Nuclear Magnetic Relaxation Dispersion (NMRD) profiles describe the efficacy of the complex in terms of relaxivity as a function of the magnetic field, and they are helpful to characterize the parameters governing proton relaxivity [37,38]. Typically, the analysis of NMRD curves allows for estimating some of the physicochemical parameters that determine relaxivity, in particular the rotational correlation time (τ_R), the water exchange rate (k_{ex}), the number of water molecules directly coordinated to Gd^{3+} (q), and the electronic relaxation rates. However, it is important to determine a maximum of these parameters independently for the reliability of the results.

In the case of TTHA complexes, as there is no water molecule directly coordinated to Gd^{3+}, the relaxivity is a sum of outer sphere and, if present, second sphere contributions [33]. The NMRD profiles of **4** and **5** were measured between 10 kHz and 400 MHz and are presented in Figure 2 and in supporting information (Figure S6 in Supplementary Materials).

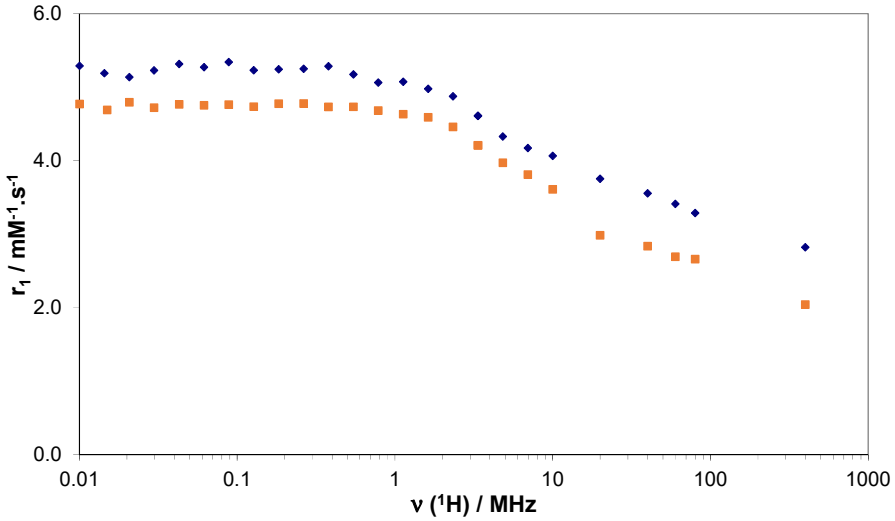

Figure 2. ^{1}H NMRD profiles of **4** (■) and **5** (♦) at 25 °C and pH = 7.0.

The low relaxivities observed are in accordance with the absence of inner sphere water molecules in the complexes. At 20 MHz, 25 °C, the relaxivities are 2.99 and 3.75 mM^{-1} s^{-1} for **4** and **5**, respectively; therefore, an increase of 25% is observed when replacing OMe by OH groups on the CDs. As the two complexes are supposed to have similar size, thus rotational dynamics, the higher relaxivity for **5** can be ascribed to the presence of second sphere water molecules contributing to the overall relaxivity, which is consistent with the presence of an H-bonding network in the case of the TTHA-substituted native CD **5**. It should be noted that rough simulations of a purely outer sphere mechanism give a relaxivity of 2.3 mM^{-1} s^{-1} at 20 MHz and 25 °C, in the same order of magnitude as that measured for **4**. This is also the value reported for GdTTHA in the same conditions [33].

2.4. Relaxometric Analysis of DOTA-Derived Complexes **1**–**3**

The NMRD profiles of **1**–**3** were also recorded between 10 kHz and 400 MHz, at 25 °C, 37 °C, and 50 °C (see Figure 3 and Figures S3–S5 in Supplementary Materials). It should be noted that the relaxivity profile of **3** was already partially measured and analyzed by Botta et al. [25], but for the sake of direct comparison, it was re-measured in identical conditions as those of **1** and **2**. The relaxivity values of **3** were similar (within 5–10%) to those previously reported.

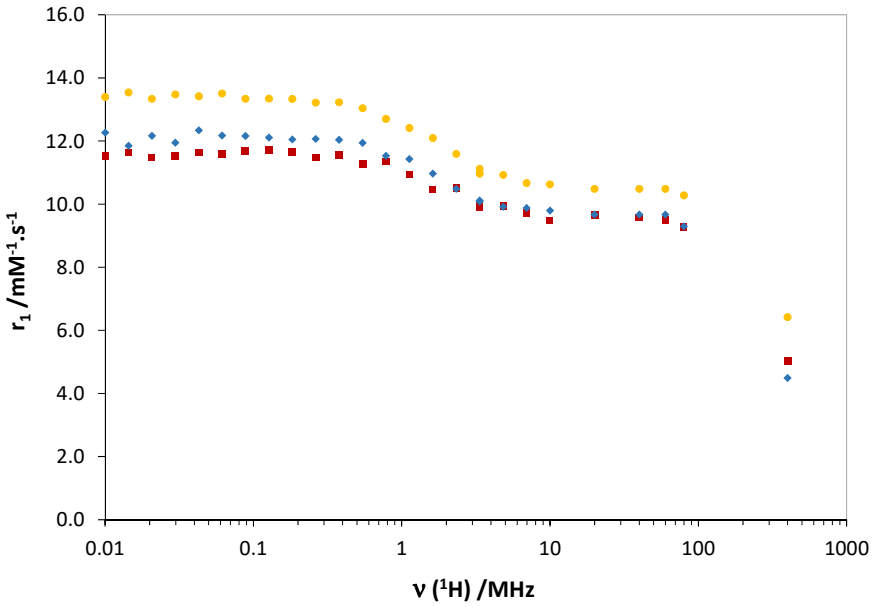

Figure 3. ^{1}H NMRD profiles of **1** (♦) **2** (●), and **3** (■) at 25 °C and pH = 7.0.

The relaxivities determined at 20 MHz and 25 °C were 9.67, 10.50, and 9.64 mM^{-1} s^{-1} for **1**, **2**, and **3**, respectively. These values are ~2.5 times higher than the relaxivity of clinically used contrast agents like GdDOTA (3.5 mM^{-1} s^{-1}). In the NMRD profiles, we note however the absence of a relaxivity "hump" at intermediate fields, which is characteristic of slowly rotating macromolecular Gd^{3+} complexes. This is also in accordance with previous data from Botta et al. [25] and us [18], and indicates that the CD-based systems are not characterized by very slow motion as they are relatively flexible, and do not aggregate in aqueous solution. The relaxivity (measured at 25 °C and 20 MHz) was found independent of the concentration (between 0.5 and 5 mM), evidencing again the absence of intermolecular interactions in this concentration range.

The relaxivity of the native CD **1** and permethylated one **3** were similar, in contrast to what had been observed previously in the case of CD substituted by TTHA derivatives **4** and **5**. A modest increase of relaxivity of ~9% was observed for the partially methylated CD **2**. On the simple assumption that a higher hydrogen bonding network would result in a higher number of second sphere water molecules contributing to relaxivity, we would have expected a relaxivity increase in the following order: **3** < **2** < **1**.

The temperature dependence of the relaxivities provides qualitative information on the parameter that limits relaxivity for a given system. Indeed, upon temperature increase, both the water exchange and the rotational dynamics become faster. If fast rotational dynamics is a limiting factor, the relaxivity will decrease upon increasing the temperature. Conversely, if relaxivity is limited by slow water exchange, increasing the temperature will lead to the acceleration of the water exchange, thus an increase in relaxivity. If slow water exchange and fast rotation are both limiting factors, as a result of an interplay between the two, relaxivity can be relatively independent of temperature. The temperature dependence of the different systems (**1**–**3**) showed similar relaxivities at 25 °C and 37 °C, whereas r_1 became lower at 50 °C (Supplementary Materials). This suggests that at the lower temperatures slow water exchange starts to become the limiting parameter, rather than fast rotational dynamics. In order to better decipher the relaxivity dependence, we performed ^{17}O NMR measurements on the different **1**–**3** complexes.

2.5. ^{17}O NMR Data of Complexes **1**–**3**

Variable temperature ^{17}O T_2 measurements give access to the water exchange rate, k_{ex}. The reduced ^{17}O transverse relaxation rates for **1**–**3** are presented in Figure 4. The behavior of **3** is classical with an increase of the reduced transverse relaxation rates (up to

~55 °C), followed by a decrease with increasing temperature, indicating that the complex is in the slow kinetic region below 55 °C. In this region, $1/T_{2r}$ is directly determined by the water exchange rate constant k_{ex}, allowing for a reliable determination of k_{ex} value. The ^{17}O data have been fitted to the Swift–Connick equations, where the number of water molecules coordinated to Gd^{3+} was fixed to 1, and the scalar coupling constant, $A/\hbar$, was fixed to -3.6×10^6 rad s^{-1}. The fit yielded a value of $k_{ex}^{298} = (1.49 \pm 0.08) \times 10^6$ s^{-1}, while $\Delta H^{\neq} = (37 \pm 3)$ kJ mol^{-1} was obtained for the activation enthalpy of the water exchange. The k_{ex}^{298} value is similar to what was previously estimated by Botta et al. from the fitting of the NMRD profile ($k_{ex}^{298} = 1.7 \times 10^6$ s^{-1}) [25], and in the same order of magnitude as water exchange rate constants typical of monoamide DOTA complexes of Gd^{3+} [7]. It is nearly three times lower than the water exchange rate of GdDOTA ($k_{ex}^{298} = 4.1 \times 10^6$), and higher than that of GdDOTAM (see Table 1), which is consistent with previous observations on analogous systems. Indeed, in the case of dissociative exchange for DOTA-derivatives (which is expected here), it is generally observed that the replacement of one negatively charged carboxylate in the complex with a neutral amide decreases the water exchange rate of about one-third [7].

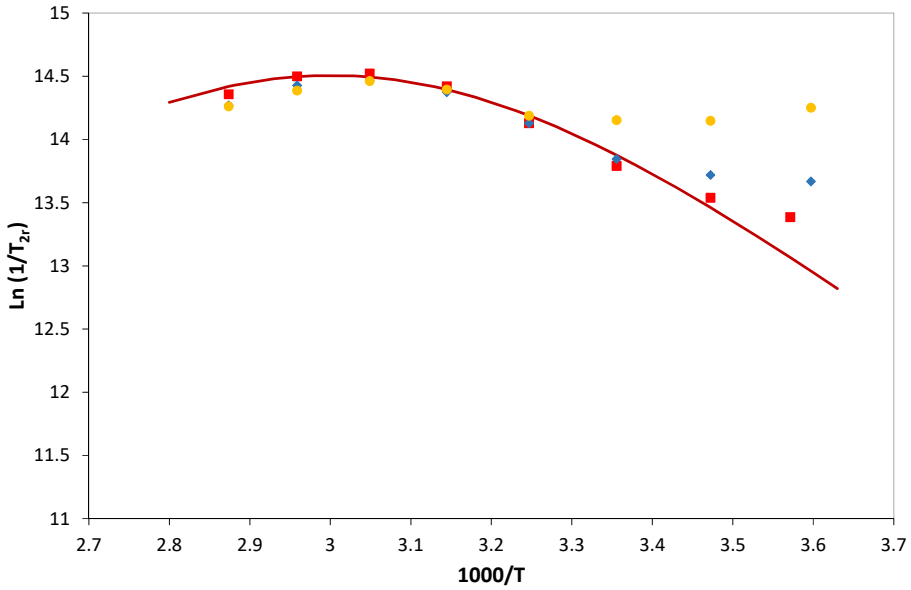

Figure 4. Temperature dependence of the reduced ^{17}O transverse relaxation rates of **1** (♦, 10.04 mM) **2** (●, 3.2 mM), and **3** (■, 10.33 mM) at 9.4 T and pH = 7.0. The continuous curve represents the best fit to the experimental data points of **3**.

Table 1. Water exchange rates (k_{ex}^{298}) of various GdDOTA derivative complexes.

	3	**3** [a]	**GdDO3A-bz-NO_2**	**Gd_2-Wazaby6**	**GdDOTA**	**GdDOTAM**
Coordinating unit	DOTA-monoamide	DOTA-monoamide	DOTA-monoamide + COO^-	DOTA-monoamide	DOTA	DOTA-tetramide
k_{ex}^{298} (10^6 s^{-1})	1.49 ± 0.08	1.7	1.6	2.8	4.1	0.053
Reference	This work	[25]	[39]	[40]	[38]	[41]

[a] Obtained from fitting of NMRD data from ref. [25].

In contrast to **3**, **1** and **2** have a very different behavior. Indeed, at low temperatures the ^{17}O $\ln(1/T_{2r})$ values are rather constant. This might be indicative of the presence of more than one species (isomers) in solution with different water exchange properties. The SAP (square antiprismatic) and TSAP (twisted square antiprismatic) isomers of macrocyclic systems such as DOTA derivatives are known to have different water exchange rate and their ratio can be very different depending on the systems [42,43]. In order to obtain information on the potential coexistence of different species in solution, we recorded ^1H NMR spectra on the corresponding Eu^{3+} complexes obtained using similar protocol as for

the Gd complexes (Figures S7 and S8 in the Supplementary Materials). Europium is the neighboring element to Gd in the lanthanide series, so they are expected to have similar coordination environment. Eu^{3+} is also paramagnetic; it causes large chemical shifts but much less line-broadening than Gd^{3+}. Unfortunately, the ^{1}H NMR spectra of the Eu^{3+} analogs of **1** and **2**, recorded at different temperatures, show broad resonances, combined with the presence of many protons of the cyclodextrins in the diamagnetic window which dominate the spectra. Overall, this prevents distinguishing different isomers. In the absence of information about the presence of different species in solution and their ratio, the analysis of the ^{17}O transverse relaxation rates could not be realized for **1** and **2**. Nevertheless, the temperature dependence of the transverse ^{17}O relaxation rates at low temperature clearly showed a very different water exchange for **1**–**3**. Although we can only speculate on the origin of this difference, it is plausible to hypothesize that it could be related to the different H-bonding network generated by the three different cyclodextrins scaffolds, which can have an influence on the water exchange rate of the Gd^{3+} complexes.

In overall, the combined ^{17}O NMR and NMRD data suggest that these highly hydrophilic systems have a complex behavior in which the hydrogen bonding network does not only contribute to a second sphere proton relaxation mechanism, but it also affects the exchange rate of the inner sphere water molecule of the Gd^{3+} complexes. The complexity of the systems prevents any reliable fit of the NMRD data.

3. Conclusions

We described β-CDs bearing derivatives of DOTA and TTHA ligands for Gd^{3+} complexation. The molecules have been obtained using novel synthetic routes. We studied the influence of the numerous hydrophilic OH groups of the CD structure, which create a strong hydrogen bonding network involving second sphere water molecules, on the proton relaxivity and on the water exchange rate of the Gd^{3+} complexes. In the absence of inner sphere water molecule in the Gd^{3+} complex (TTHA ligand), the relaxivity increases with the increasing number of hydroxyl groups on the CD, confirming a strong second sphere contribution to the relaxivity, induced by the hydrophilicity of the molecule. In the case of DOTA derivatives, the situation is more complicated. Indeed, the variation of the relaxivity between the systems containing a different number of OH groups on the CD is not guided by the increase of hydroxyl functions. ^{17}O NMR measurements revealed different water exchange processes depending on the number of hydroxyls on the CD. For the permethylated system **3**, a classical water exchange rate is found, consistent with typical GdDOTA-monoamide complexes. In contrast, when hydroxyls are present on the CD **1** and **2**, the water exchange process becomes clearly different, as evidenced by ^{17}O T_2 data. These different water exchange properties will very likely impact the relaxivity. In overall, these highly hydrophilic systems have a hydrogen-bound network that induces a second sphere relaxivity, but it also influences the water exchange process. Altogether this leads to a complicated relaxation behavior.

Supplementary Materials: The materials, method, synthesis, and characterization details of products **7**, **9**, **12**, **15**–**21**, **23**–**29**, **1**–**5**, and europium complexes are available online at https://www.mdpi.com/2227-9717/9/2/269/s1. ^{1}H NMRD profiles of contrast agents **1**–**4** at 25 °C, 37 °C, and ^{1}H NMR spectra of europium complexes of **24** and **25** at 9.4 T and 5 °C, 25 °C, and 37 °C are also reported.

Author Contributions: Conceptualization, G.G. and F.E.; Methodology, G.G., F.E., É.T., and C.S.B.; Validation, G.G., F.E., É.T., and C.S.B.; Formal Analysis, A.B., B.-S.S.-B., S.B., M.B., C.B., A.P. and C.S.B.; Investigation, A.B., B.-S.S.-B., S.B., M.B., C.B., and A.P.; Writing—Original draft preparation G.G. and C.S.B.; Writing—review and editing, F.E. and É.T.; Supervision, G.G., F.E., S.B., C.S.B., and É.T.; Project administration, Funding acquisition, G.G. All authors have read and agreed to the published version of the manuscripts.

Funding: This research was funded by the Interreg IV AI-Chem Channel (PhD A.B.).

Institutional Review Board Statement: Not applicable.

Informed Consent Statement: Not applicable.

Data Availability Statement: No data.

Acknowledgments: We thank Raphaël Tripier from UMR 6521, University of Bretagne Occidentale (Brest) for sending some tri*tert*butylDOTA **13**. We are also grateful for the compagny Cyclolab, https://cyclolab.hu/, for its contribution by sending β-CD-NH_2 **10**.

Conflicts of Interest: The authors declare no conflict of interest.

References

1. Caravan, P.; Ellison, J.J.; McMurry, T.J.; Lauffer, R.B. Gadolinium(III) Chelates as MRI Contrast Agents: Structure, Dynamics, and Applications. *Chem. Rev.* **1999**, *99*, 2293–2352. [CrossRef] [PubMed]
2. Aime, S.; Botta, M.; Terreno, E. Gd(III)-based contrast agents for MRI. *Adv. Inorg. Chem.* **2005**, *57*, 173–237. [CrossRef]
3. Hermann, P.; Kotek, J.; Kubícek, V.; Lukes, I. Gadolinium(III) Complexes as MRI Contrast Agents: Ligand Design and Properties of the Complexes. *Dalton Trans.* **2008**, *23*, 3027–3047. [CrossRef] [PubMed]
4. Botta, M. Second Coordination Sphere Water Molecules and Relaxivity of Gadolinium(III) Complexes: Implications for MRI Contrast Agents. *Eur. J. Inorg. Chem.* **2000**, *2000*, 399–407. [CrossRef]
5. Rudovsky, J.; Kotek, J.; Hermann, P.; Lukes, I.; Mainero, V.; Aime, S. Synthesis of a bifunctional monophosphinic acid DOTA analogue ligand and its lanthanide(III) complexes. A gadolinium(III) complex endowed with an optimal water exchange rate for MRI applications. *Org. Biomol. Chem.* **2005**, *3*, 112–117. [CrossRef] [PubMed]
6. Bonnet, C.S.; Fries, P.H.; Crouzy, S.; Delangle, P. Outer-Sphere Investigation of MRI Relaxation Contrast Agents. Example of a Cyclodecapeptide Gadolinium Complex with Second-Sphere Water. *J. Phys. Chem. B* **2010**, *114*, 8770–8781. [CrossRef]
7. Merbach, A.; Helm, L.; Toth, E. *The Chemistry of Contrast Agents in Medical Magnetic Resonance Imaging*, 2nd ed.; Wiley: Hoboken, NJ, USA; Chichester, UK, 2013. [CrossRef]
8. Solomon, I.; Bloembergen, N. Nuclear Magnetic Interactions in the HF Molecule. *J. Chem. Phys.* **1956**, *25*, 261–266. [CrossRef]
9. Bloembergen, N.; Morgan, L.O. Proton Relaxation Times in Paramagnetic Solutions. Effects of Electron Spin Relaxation. *J. Chem. Phys.* **1961**, *34*, 842–850. [CrossRef]
10. Idée, J.-M.; Port, M.; Medina, C.; Lancelot, E.; Fayoux, E.; Ballet, S.; Corot, C. Possible Involvement of Gadolinium Chelates in the Pathophysiology of Nephrogenic Systemic Fibrosis: A Critical Review. *Toxicology* **2008**, *248*, 77–88. [CrossRef]
11. Port, M.; Idée, J.-M.; Medina, C.; Robic, C.; Sabatou, M.; Corot, C. Efficiency, thermodynamic and kinetic stability of marketed gadolinium chelates and their possible clinical consequences: A critical review. *Biometals* **2008**, *21*, 469–490. [CrossRef]
12. Fraum, T.J.; Ludwig, D.R.; Bashir, M.R.; Kathryn, J.F. Toxicity Gadolinium-Based Contrast Agents: A Comprehensive Risk Assessment: Gadolinium Risk Assessment. *J. Magn. Reson. Imaging* **2017**, *46*, 338–353. [CrossRef] [PubMed]
13. Sieving, P.F.; Watson, A.D.; Roklage, S.M. Preparation and Characterization of Paramagnetic Polychelates and Their Protein Conjugates. *Bioconjugate Chem.* **1990**, *1*, 65–71. [CrossRef] [PubMed]
14. Tóth, E.; Connac, F.; Helm, L.; Adzamli, K.; Merbach, A.E. Direct assessment of water exchange on a Gd(III) chelate bound to a protein. *J. Biol. Inorg. Chem.* **1998**, *3*, 606–613. [CrossRef]
15. Zech, S.G.; Eldredge, H.B.; Lowe, M.P.; Caravan, P. Protein Binding to Lanthanide(III) Complexes Can Reduce the Water Exchange Rate at the Lanthanide. *Inorg. Chem.* **2007**, *46*, 3576–3584. [CrossRef]
16. Rudovsky, J.; Botta, M.; Hermann, P.; Hardcastle, K.I.; Lukes, I.; Aime, S. PAMAM Dendrimeric Conjugates with a Gd-DOTA Phosphinate Derivative and Their Adducts with Polyaminoacids: The Interplay of Global Motion, Internal Rotation, and Fast Water Exchange. *Bioconjugate Chem.* **2006**, *17*, 975–987. [CrossRef] [PubMed]
17. Champagne, P.-L.; Barbot, C.; Zhang, P.; Han, X.; Gaamoussi, I.; Hubert-Roux, M.; Bertolesi, G.E.; Gouhier, G.; Ling, C.-C. Synthesis and Unprecedented Complexation Properties of β-Cyclodextrin-Based Ligand for Lanthanide Ions. *Inorg. Chem.* **2018**, *57*, 8964–8977. [CrossRef]
18. Fredy, J.W.; Scelle, J.; Guenet, A.; Morel, E.; Adam de Beaumais, S.; Menand, M.; Marvaud, V.; Bonnet, C.S.; Toth, E.; Sollogoub, M.; et al. Cyclodextrin Polyrotaxanes as a Highly Modular Platform for the Development of Imaging Agents. *Chem. Eur. J.* **2014**, *20*, 10915–10920. [CrossRef]
19. Fredy, J.W.; Scelle, J.; Ramniceanu, G.; Doan, B.-T.; Bonnet, C.S.; Tóth, É.; Ménand, M.; Sollogoub, M.; Vives, G.; Hasenknopf, B. Mechanostereoselective One-Pot Synthesis of Functionalized Head-to-Head Cyclodextrin [3] Rotaxanes and Their Application as Magnetic Resonance Imaging Contrast Agents. *Org. Lett.* **2017**, *19*, 1136–1139. [CrossRef]
20. Mondjinou, Y.A.; Loren, B.P.; Collins, C.J.; Hyun, S.-H.; Demoret, A.; Skulsky, J.; Chaplain, C.; Badwaik, V.; Thompson, D.H. Gd3+: DOTA-Modified 2-Hydroxypropyl-β-Cyclodextrin/4-Sulfobutyl Ether-β-Cyclodextrin-Based Polyrotaxanes as Long Circulating High Relaxivity MRI Contrast Agents. *Bioconjugate Chem.* **2018**, *29*, 3550–3560. [CrossRef]
21. D'Souza, V.T.; Lipkowitz, K.B. Cyclodextrins: Introduction. *Chem. Rev.* **1998**, *98*, 1741–1742. [CrossRef]
22. Aime, S.; Gianolio, E.; Terreno, E.; Menegotto, I.; Bracco, C.; Milone, L.; Cravotto, G. β-Cyclodextrin adducts of Gd(III) chelates: Useful models for investigating the structural and dynamic determinants of the relaxivity of gadolinium-based systems. *Magn. Reson. Chem.* **2003**, *41*, 800–805. [CrossRef]

23. Aime, S.; Gianolio, E.; Arena, F.; Alessandro Barge, A.; Martina, K.; Heropoulos, G.; Cravotto, G. New cyclodextrin dimers and trimers capable of forming supramolecular adducts with shape-specific ligands. *Org. Biomol. Chem.* **2009**, *7*, 370–379. [CrossRef] [PubMed]
24. Cao, Y.; Zu, G.; Kuang, Y.; He, Y.; Mao, Z.; Liu, M.; Xiong, D.; Pei, R. Biodegradable Nanoglobular Magnetic Resonance Imaging Contrast Agent Constructed with Host-Guest Self-Assembly for Tumor-Targeted Imaging. *ACS Appl. Mater. Interfaces* **2018**, *10*, 26906–26916. [CrossRef] [PubMed]
25. Skinner, P.J.; Beeby, A.; Dickins, R.S.; Parker, D.; Aime, S.; Botta, M. Conjugates of cyclodextrins with charged and neutral macrocyclic europium, terbium and gadolinium complexes: Sensitized luminescence and relaxometric investigations and an example of supramolecular relaxivity enhancement. *J. Chem. Soc. Perkin Trans.* **2000**, *2*, 1329–1338. [CrossRef]
26. Hana, Y.; Qian, Y.; Zhoub, X.; Hub, H.; Liua, X.; Zhoua, Z.; Tanga, J.; Shena, Y. Biodegradable Nanoglobular Magnetic Resonance Imaging Contrast Agent Constructed with Host-Guest Self-Assembly for Tumor-Targeted Imaging. *Polym. Chem.* **2016**, *7*, 6354–6362. [CrossRef]
27. Bonnet, C.; Gadelle, A.; Pecaut, J.; Friesa, P.H.; Delangle, P. Inclusion complexes of trivalent lutetium cations with an acidic derivative of per(3,6-anhydro)-α-cyclodextrin. *Chem. Commun.* **2005**, *5*, 625–627. [CrossRef] [PubMed]
28. Bonnet, C.S.; Fries, P.H.; Gadelle, A.; Gambarelli, S.; Delangle, P. A Rigorous Framework to Interpret Water Relaxivity. The Case Study of a Gd(III) Complex with an α-Cyclodextrin Derivative. *J. Am. Chem. Soc.* **2008**, *130*, 10401–10413. [CrossRef]
29. Battistini, E.; Gianolio, E.; Gref, R.; Couvreur, P.; Fuzerova, S.; Othman, M.; Aime, S.; Badet, B.; Durand, P. High-Relaxivity Magnetic Resonance Imaging (MRI) Contrast Agent Based on Supramolecular Assembly between a Gadolinium Chelate, a Modified Dextran, and Poly-β-Cyclodextrin. *Chem. Eur. J.* **2008**, *14*, 4551–4561. [CrossRef]
30. Idriss, H.; Estour, F.; Zgani, I.; Barbot, C.; Biscotti, A.; Petit, S.; Galaup, C.; Hubert-Roux, M.; Nicol, L.; Mulder, P.; et al. Effect of the Second Coordination Sphere on New Contrast Agents Based on Cyclodextrin Scaffolds for MRI Signals. *RSC Adv.* **2013**, *3*, 4531–4534. [CrossRef]
31. Zgani, I.; Idriss, H.; Barbot, C.; Djedaïni-Pilard, F.; Petit, S.; Hubert-Roux, M.; Estour, F.; Gouhier, G. Positive Variation of the MRI Signal via Intramolecular Inclusion Complexation of a C-2 Functionalized β-Cyclodextrin. *Org. Biomol. Chem.* **2017**, *15*, 564–569. [CrossRef]
32. Biscotti, A.; Barbot, C.; Nicol, L.; Mulder, P.; Sappei, C.; Hubert-Roux, M.; Déchamps-Olivier, I.; Estour, F.; Gouhier, G. MRI probes based on C6-peracetate β-cyclodextrins: Synthesis, gadolinium complexation and in vivo relaxivity studies. *Polyhedron* **2018**, *148*, 32–43. [CrossRef]
33. Zitha-Bovens, E.; Muller, R.N.; Laurent, S.; Vander, E.L.; Geraldes, C.F.G.C.; van Bekkum, H.; Peters, J.A. Structure and Dynamics of Lanthanide Complexes of Triethylenetetramine-*N*, *N*, *N′*, *N′′*, *N′′′*, *N′′′*-hexaacetic Acid (H_6ttha) and of Diamides H_4ttha (NHR) Derived from H_6ttha as Studied by NMR, NMRD, and EPR. *Helv. Chim. Acta* **2005**, *88*, 618–632. [CrossRef]
34. Martinelli, J.; Thangavel, K.; Tei, L.; Botta, M. Dendrimeric b-Cyclodextrin/GdIII Chelate SupramolecularHost–Guest Adducts as High-Relaxivity MRI Probes. *Chem. Eur. J.* **2014**, *20*, 10944–10952. [CrossRef] [PubMed]
35. Laakso, J.; Rosser, G.A.; Szíjjártó, C.; Beeby, A.; Borbas, K.E. Synthesis of Chlorin-Sensitized Near Infrared-Emitting Lanthanide Complexes. *Inorg. Chem.* **2012**, *51*, 10366–10374. [CrossRef]
36. Montalbetti, C.A.G.N.; Falque, V. Amide bond formation and peptide coupling. *Tetrahedron* **2005**, *61*, 10827–10852. [CrossRef]
37. Swift, T.J.; Connick, R.E. NMR Relaxation Mechanisms of O^{17} in Aqueous Solutions of Paramagnetic Cations and the Lifetime of Water Molecules in the First Coordination Sphere. *J. Chem. Phys.* **1962**, *37*, 307–320. [CrossRef]
38. Powell, D.H.; Ni Dhubhghaill, O.M.; Pubanz, D.; Helm, L.; Lebedev, Y.S.; Schlaepfer, W.; Merbach, A.E. Structural and Dynamic Parameters Obtained from ^{17}O NMR, EPR, and NMRD Studies of Monomeric and Dimeric Gd^{3+} Complexes of Interest in Magnetic Resonance Imaging: An Integrated and Theoretically Self-Consistent Approach. *J. Am. Chem. Soc.* **1996**, *118*, 9333–9346. [CrossRef]
39. Tóth, É.; Pubanz, D.; Vauthey, S.; Helm, L.; Merbach, A.E. The Role of Water Exchange in Attaining Maximum Relaxivities for Dendrimeric MRI Contrast Agents. *Chem. Eur. J.* **1996**, *2*, 1607–1615. [CrossRef]
40. Florès, O.; Pliquett, J.; Galan, L.A.; Lescure, R.; Denat, F.; Maury, O.; Pallier, A.; Bellaye, P.-S.; Collin, B.; Même, S.; et al. Aza-BODIPY Platform: Toward an Efficient Water-Soluble Bimodal Imaging Probe for MRI and Near-Infrared Fluorescence. *Inorg. Chem.* **2020**, *59*, 1306–1314. [CrossRef]
41. Aime, S.; Barge, A.; Bruce, J.I.; Botta, M.; Howard, J.A.K.; Moloney, J.M.; Parker, D.; De Sousa, A.S.; Woods, M. NMR, Relaxometric, and Structural Studies of the Hydration and Exchange Dynamics of Cationic Lanthanide Complexes of Macrocyclic Tetraamide Ligands. *J. Am. Chem. Soc.* **1999**, *121*, 5762–5771. [CrossRef]
42. Aime, S.; Barge, A.; Botta, M.; De Sousa, A.S.; Parker, P. Direct NMR Spectroscopic Observation of a Lanthanide-Coordinated Water Molecule whose Exchange Rate Is Dependent on the Conformation of the Complexes. *Angew. Chem. Int. Ed.* **1998**, *37*, 2673–2675. [CrossRef]
43. Platas-Iglesias, C. The Solution Structure and Dynamics of MRI Probes Based on Lanthanide(III) DOTA as Investigated by DFT and NMR Spectroscopy. *Eur. J. Inorg. Chem.* **2012**, *12*, 2023–2033. [CrossRef]